ACADEMIC PRESS

Available online at www.sciencedirect.com
SCIENCE DIRECT®

NeuroImage

NeuroImage 20 (2003) 1411–1418

www.elsevier.com/locate/ynimg

Technical Report

k-Space based summary motion detection for functional magnetic resonance imaging

Elisabeth C. Caparelli,[a,*] Dardo Tomasi,[a,b] Sheeba Arnold,[a] Linda Chang,[a] and Thomas Ernst[a]

[a] *Medical Department, Brookhaven National Laboratory, Upton, NY 11973, USA*
[b] *Escuela de Ciencia y Tecnologia, Universidad Nacional de General San Martin, Alem 3901, 1651 V. Ballester, Buenos Aires, Argentina*

Received 13 January 2003; revised 16 May 2003; accepted 29 May 2003

Abstract

Functional MRI studies are very sensitive to motion; head movements of as little as 1-mm translations or 1° rotations may cause spurious signals. An algorithm was developed that uses *k*-space MRI data to monitor subject motion during functional MRI time series. A *k*-space weighted average of squared difference between the initial scan and subsequent scans is calculated, which summarizes subject motion in a single quality parameter; however, the quality parameter cannot be used for motion correction. The evolution of this quality parameter throughout a time series indicates whether head motion is within a predetermined limit. Fifty functional MRI studies were used to calibrate the sensitivity of the algorithm, using the six rigid-body registration parameters (three translations and three rotations) from the statistical parametric mapping (SPM99) package as a reference. The average correlation coefficient between the new quality parameter and the reference value from SPM was 0.84. The simple algorithm correctly classified acceptable or excessive motion with 90% accuracy, with the remaining 10% being borderline cases. This method makes it possible to evaluate brain motion within seconds after a scan and to decide whether a study needs to be repeated.
© 2003 Elsevier Inc. All rights reserved.

Keywords: fMRI; Brain movement; Motion detector; *k*-space data

Introduction

Functional MRI (fMRI) with blood oxygenation level dependence (BOLD) contrast relies on the detection of signal changes as a result of brain activation. T_2*-weighted images are commonly used because they are most sensitive to the BOLD effect. However, even under optimal conditions and high magnetic field strengths, BOLD signal changes are very small (typically 1–5%), so that head motion may easily corrupt the results of activation studies (Friston et al., 1996). Therefore, it is important to realign fMRI time series prior to statistical analysis. However, even with motion correction, the range of acceptable motion is on the order of a few millimeters of translation and a few degrees of rotation, and scans with a greater range of motion are rejected by many research groups. With such a small range of acceptable motion, a significant amount of individual scans, or even entire scanning sessions, may have to be discarded, especially in fMRI studies of children or sick adults.

One potential solution to this problem is motion correction in real time, using changes in reconstructed images from scan to scan to calculate and correct for motion in subsequent scans. Because fMRI studies are performed with repetition times of a few seconds, these real time methods require powerful computers to determine motion parameters in real time and may only work for small movements. For example, a recent publication presented an improved method where translations up to 2 mm could be partially corrected in real time (Mathiak and Posse, 2001). Another approach is to determine motion from a navigator echo scan

* Corresponding author. Brookhaven National Laboratory, Medical Department, Building 490, Upton, NY 11973, USA. Fax: +1-631-344-7671.

E-mail address: caparelli@bnl.gov (E.C. Caparelli).

1053-8119/03/$ – see front matter © 2003 Elsevier Inc. All rights reserved.
doi:10.1016/S1053-8119(03)00339-2

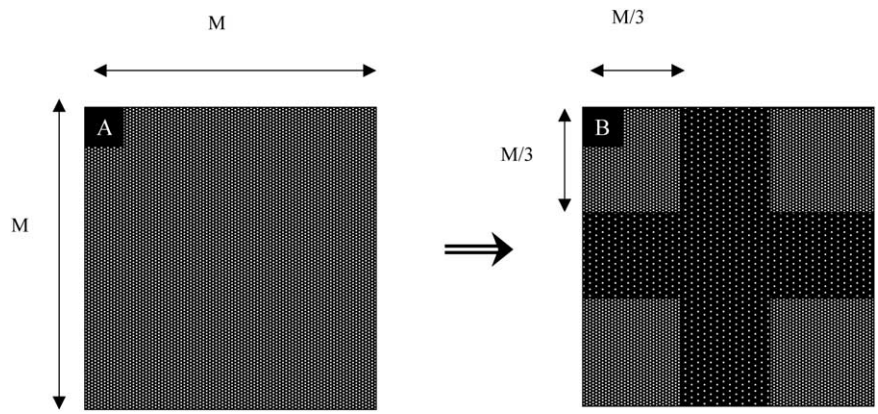

Fig. 1. (A) 2D square matrix of size $M \times M$; (B) The same data matrix showing the four square corner regions (size $M/3 \times M/3$) that are used to calculate the quality measures $A(t)$ and $A'(t)$ defined in Eqs. (7) and (8).

that is acquired before each volume scan. The use of three orthogonal orbital *k*-space trajectories was found to be inaccurate for *z*-translations above 1 mm and coronal rotations greater than 1.5° (Ward et al., 2000). More recently, a 3D spherical navigator echo has been proposed, which samples a spherical shell of *k*-space centered at the origin and which allows accurate determination of displacements up to 5 mm and 6° (Welch et al., 2002).

Even if large movements can be determined accurately, current prospective and retrospective motion correction techniques generally correct only for geometric rigid-body effects, although recent approaches also remove some geometric distortions due to motion (Jenkinson et al., 2002). However, subject motion may also cause nongeometric and generally nonlinear changes in the BOLD signal, such as changes in effective shim due to motion (Thesen et al., 2000; Jezzard and Balaban, 1995), temporary changes in the spin history (Friston et al., 1996; Robson et al., 1997), and changes in local susceptibility due to motion (Wu et al., 1997). Furthermore, real time motion correction algorithms are not generally available yet. Therefore, current in vivo fMRI studies are limited to scans with very small degrees of motion.

During the course of several ongoing fMRI studies, we found that a significant number of scans (over 50%) did not meet our internal quality criteria of 1-mm translations and 1° rotations. Because existing motion-estimation algorithms, such as that in the SPM package (Friston et al., 1995), are currently too slow to estimate motion in real time, many fMRI studies were lost or required repeat scans on different days. Therefore, a fast, noniterative algorithm was developed to quantify subject motion immediately after each scan. Furthermore, because our experimental MRI system does not provide real time image reconstruction, the motion-estimation algorithm uses the raw (*k*-space) data. The

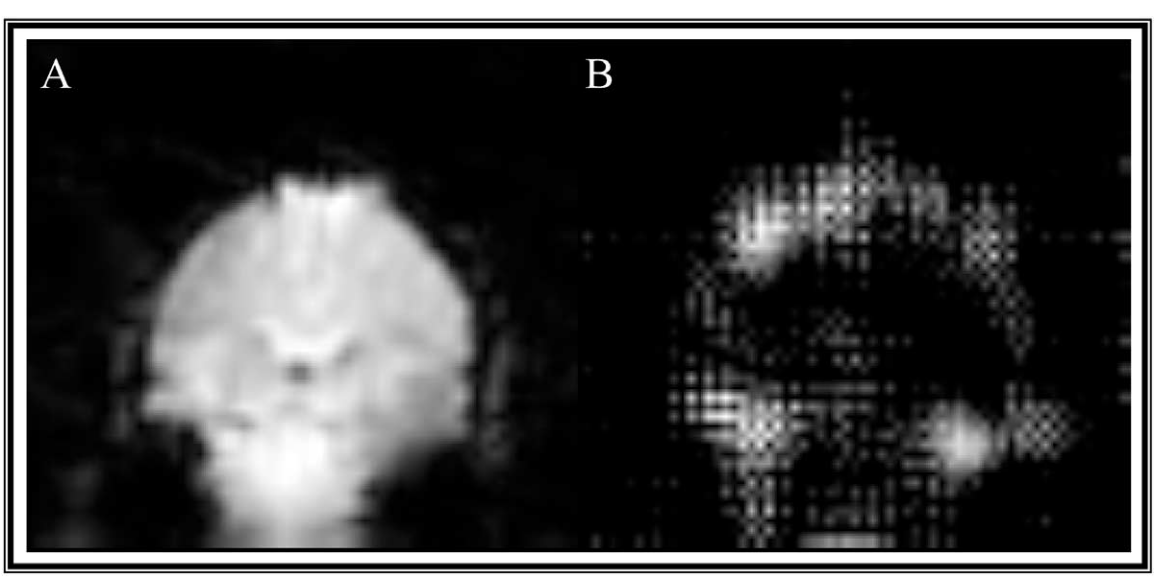

Fig. 2. (A) Original image using full *k*-space; (B) Image reconstructed using modified *k*-space data, with the center of *k*-space zeroed according to Fig. 1B.

algorithm calculates a single quality parameter for each time point, by determining a *k*-space weighted squared difference between the first and each of the subsequent time points, which summarizes and quantifies subject motion. Using 50 in vivo fMRI scans, the motion parameter was calibrated relative to the six motion parameters from SPM99 to indicate scans with subject motion above 1-mm translations or 1° rotations.

Methods

True motion parameters for fMRI time series, such as the three translations and three rotations describing rigid-body motion, can be determined with registration techniques. However, registration algorithms are computationally expensive and difficult to perform in real time. Because we were only interested in a quality measure of motion, not geometric motion parameters per se, the goal was to derive a scalar value that is sensitive to motion and can be calculated directly from *k*-space data.

Difference MR images (after reconstruction) that reflect pixel-by-pixel changes in signal intensity over time are very sensitive to motion, and increased motion generally results in greater differences. Due to the linearity between complex image space and *k*-space, the same should be true for *k*-space data. Small amounts of motion (subpixel or on the order of a few pixels) generally enhance image areas in physical space that show rapid spatial variations in image intensity, whereas areas with slowly varying image intensity are relatively unaffected by small movements. Correspondingly, in *k*-space, small amounts of motion should mostly affect the outer components of *k*-space, but leave the center of *k*-space relatively intact. This can be shown mathematically. If $I(\mathbf{x})$ represents the frequency (physical) domain signal at planar position $\mathbf{x} = (x, y)$, i.e., the "image," and $\mathcal{S}_0(\mathbf{k})$ the respective time domain signal with $\mathbf{k} = (k_x, k_y)$, then the 2D Fourier transform that relates $I(\mathbf{x})$ and $\mathcal{S}_0(\mathbf{k})$ is given by (Gradshteyn and Ryzhik, 1980)

$$\mathcal{S}_0(\mathbf{k}) = \frac{1}{2\pi}\int_{-\infty}^{\infty} I(\mathbf{x})\exp\{i\mathbf{k}\cdot\mathbf{x}\}d\mathbf{x}. \quad (1)$$

If we assume that the motion is rigid-body and is instantaneous (that is, does not occur during readout), the signal $\mathcal{S}(\mathbf{k}, \mathbf{h}, \theta)$ for a rotated and displaced image $I(\mathcal{R}(\theta)\mathbf{x} - \mathbf{h})$ can be written as

$$\begin{aligned}\mathcal{S}(\mathbf{k}, \mathbf{h}, \theta) &= \frac{1}{2\pi}\int_{-\infty}^{\infty} I(\mathcal{R}(\theta)\mathbf{x} - \mathbf{h})\exp\{i\mathbf{k}\cdot\mathbf{x}\}d\mathbf{x} \\ &= \frac{1}{2\pi}\int_{-\infty}^{\infty} I(\mathbf{x})\exp\{i\mathbf{k}\cdot\mathcal{R}^{-1}(\theta)(\mathbf{x}+\mathbf{h})\}d\mathbf{x}, \quad (2)\end{aligned}$$

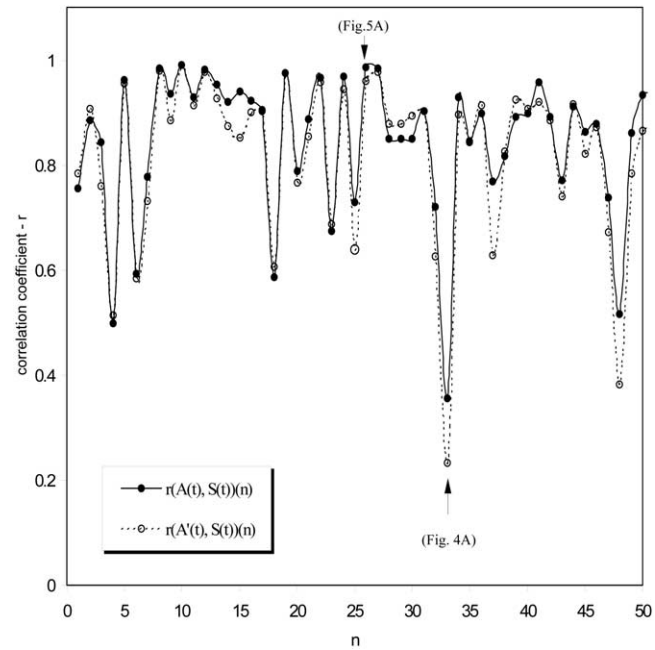

Fig. 3. Correlation coefficients between each of the two proposed motion detector measures, $A(t)$ and $A'(t)$, and the total of SPM parameters, $S(t)$, for all 50 fMRI studies. The arrows indicate the specific time series that are displayed in Figs. 4 and 5.

where $\mathbf{h} = (h_x, h_y)$ is a time-dependent displacement vector and $\mathcal{R}(\theta) = \begin{pmatrix} \cos\theta & \sin\theta \\ -\sin\theta & \cos\theta \end{pmatrix}$ is a time-dependent rotation matrix.

For small rotations $(\theta \ll 1)$, $\mathcal{R}^{-1}(\theta) \cong \mathcal{I} + \theta\mathcal{M}$, where $\mathcal{I}$ is the 2×2 identity matrix and $\mathcal{M} = \begin{pmatrix} 0 & -1 \\ 1 & 0 \end{pmatrix}$ and thus

$$\mathcal{S}(\mathbf{k}, \mathbf{h}, \theta) \cong \frac{\exp\{i\mathbf{k}\cdot\mathbf{h}\}\exp\{i\theta\mathbf{k}\cdot\mathcal{M}\mathbf{h}\}}{2\pi}\int_{-\infty}^{\infty} I(\mathbf{x}) \times \exp\{i\theta\mathbf{k}\cdot\mathcal{M}\mathbf{x}\}\exp\{i\mathbf{k}\cdot\mathbf{x}\}d\mathbf{x}. \quad (3)$$

Of note, translations $\mathbf{h}$ affect only the phase, but not the amplitude, of the *k*-space signals, whereas rotations affect both the phase and the amplitude. If we additionally assume small displacements $(\mathbf{k}\cdot\mathbf{h} \ll 1)$, and include only first-order terms in $\mathbf{k}$, θ, and $\mathbf{h}$, we obtain

$$\mathcal{S}(\mathbf{k}, \mathbf{h}, \theta) \cong (1 + i\mathbf{k}\cdot\mathbf{h})\mathcal{S}_0(\mathbf{k}) + i\theta\mathbf{k}\cdot\mathcal{S}_1(\mathbf{k}), \quad (4)$$

where

$$\mathcal{S}_1(\mathbf{k}) = \frac{1}{2\pi}\int_{-\infty}^{\infty} I(\mathbf{x})\mathcal{M}\mathbf{x}\exp\{i\mathbf{k}\cdot\mathbf{x}\}d\mathbf{x}. \quad (5)$$

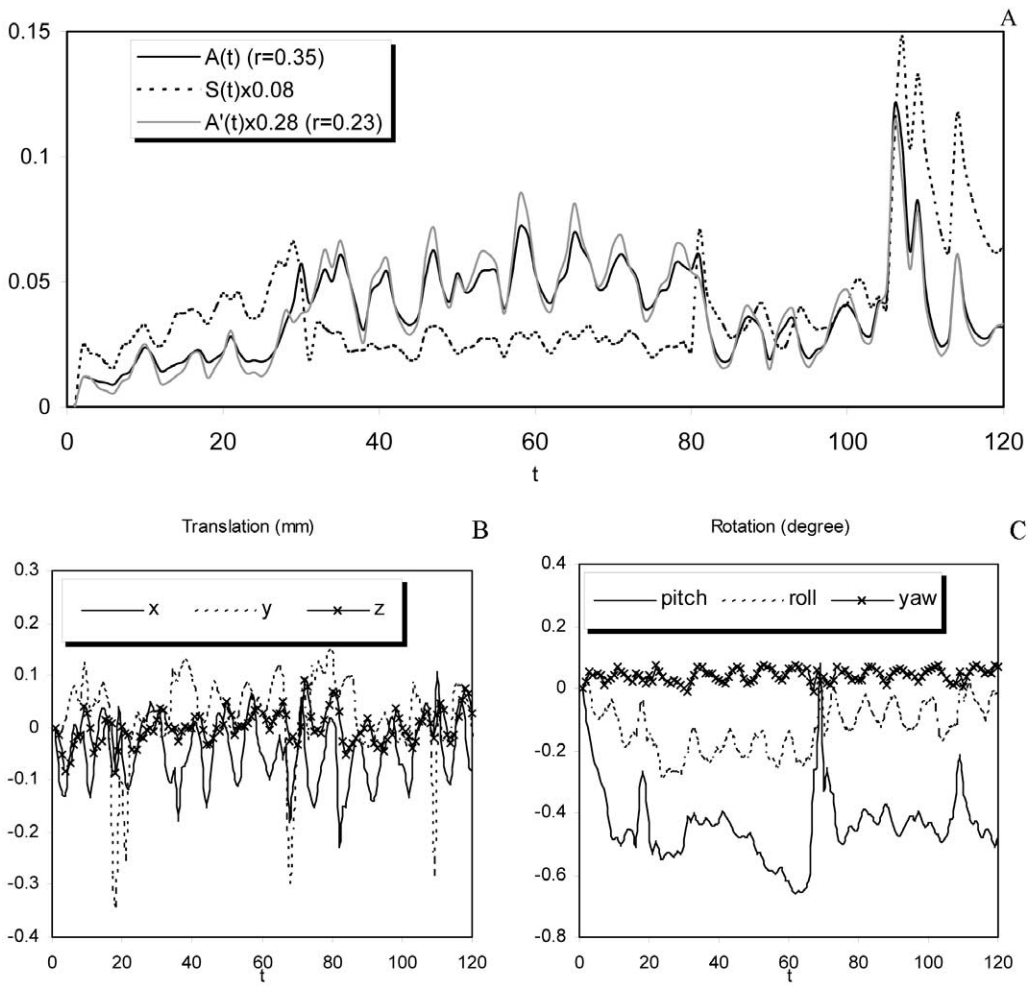

Fig. 4. (A) Evolution of the quality parameters $A(t)$ and $A'(t)$ (defined in Eqs. (7) and (8)) and the total of SPM result, $S(t)$, during a scan with acceptable motion; $A'(t)$ and $S(t)$ are rescaled. (B) and (C) show the six parameters for translation and rotation determined by the SPM registration package.

As a result, the relative signal change for a given point in k-space is

$$\frac{\mathcal{S}(\mathbf{k},\ \mathbf{h},\ \theta) - \mathcal{S}_0(\mathbf{k})}{\mathcal{S}_0(\mathbf{k})} \approx i\mathbf{k} \cdot \left(\mathbf{h} + \theta\,\frac{\mathcal{S}_1(\mathbf{k})}{\mathcal{S}_0(\mathbf{k})}\right). \qquad (6)$$

This proves that the relative signal change at the center of k-space is negligible for small enough movements θ and $\mathbf{h}$.

Therefore, we hypothesized that a k-space based measure representing small movements might be designed by evaluating the difference in raw data between time points, with exclusion of the center lines and columns of the k-space, since the regions are insensitive to small movements according to Eq. (6). Specifically, the k-space (size $M \times M$) was divided into nine identical squares (each of size $M/3 \times M/3$), and only the four "corners" were included in the calculation (Fig. 1). As expected, images reconstructed with this modified data matrix (with center rows and columns set to zero) essentially contain information only close to the edges (Fig. 2).

To quantify the amount of movement in a time series of 3D acquisitions, we define the quality measure $A(t)$, which reflects the sum of squared differences between a data set acquired at time t and a reference data set acquired at $t = 0$, normalized by the sum of squares of all elements of the reference data set:

$$A(t) = \frac{\sum_{k=-N/2}^{N/2} \sum_{i,j=-M/2}^{M/2} \lambda(\mathbf{i},\ \mathbf{j})(|k_{ijk}(t)| - |k_{ijk}(0)|)^2}{\sum_{k=-N/2}^{N/2} \sum_{i,j=-M/2}^{M/2} \lambda(\mathbf{i},\ \mathbf{j})|k_{ijk}(0)|^2}, \qquad (7)$$

with

$$\lambda(i,\ j) = \begin{cases} 0 & \text{for } -M/6 < i < M/6 \\ & \quad \text{or } -M/6 < j < M/6 \\ 1 & \text{else} \end{cases}.$$

Here, $|k_{ijk}(t)|$ is the absolute value of each element of the 3D raw data matrix, which consists of N slices of an $M \times$

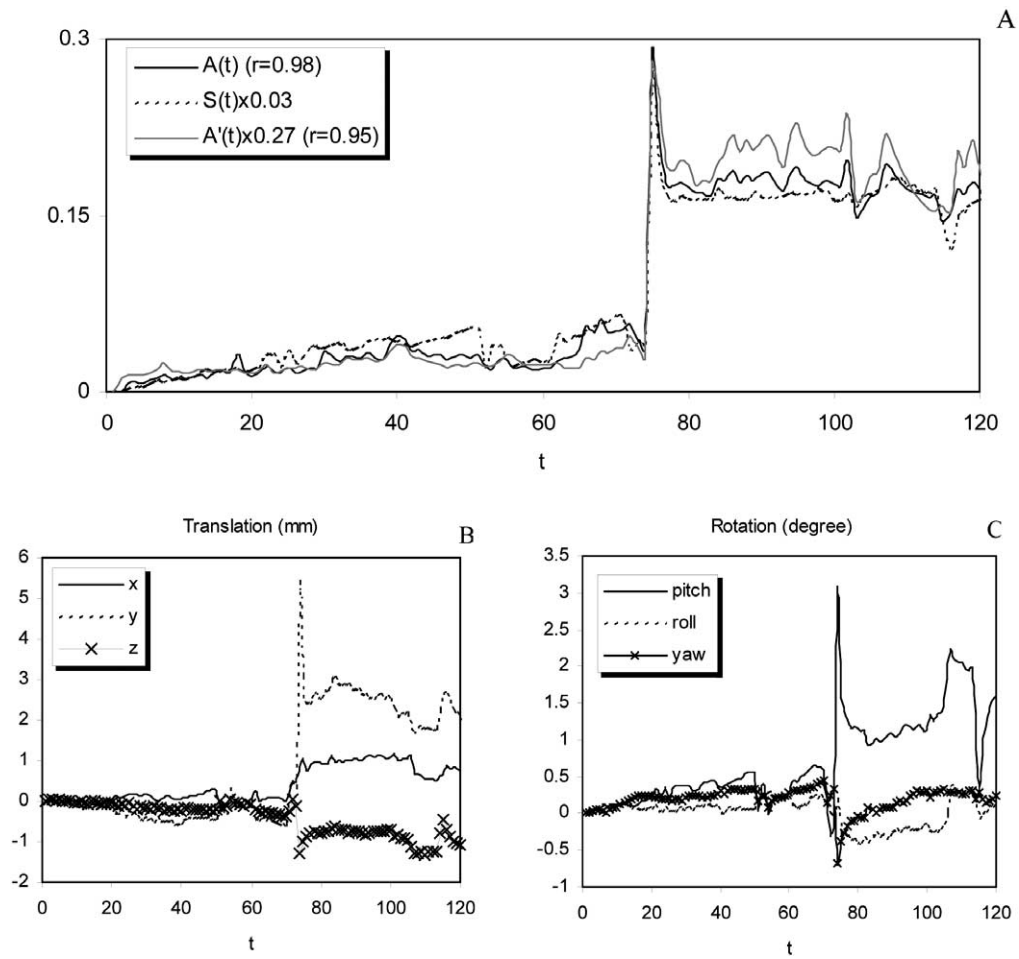

Fig. 5. (A) Evolution of the quality parameters $A(t)$ and $A'(t)$ (defined in Eqs. (7) and (8)) and the total of the SPM result, $S(t)$, during a scan with excessive motion; $A'(t)$ and $S(t)$ are rescaled. (B) and (C) show the six parameters for translation and rotation from the SPM registration package.

M k-space matrix. We also evaluated an alternative form of the quality function, $A'(t)$, in which the difference between elements of k-space was computed using complex values:

$$A'(t) = \frac{\sum_{k=-N/2}^{N/2} \sum_{i,j=-M/2}^{M/2} \lambda(\mathbf{i}, \mathbf{j}) \left| k_{ijk}(t) - k_{ijk}(0) \right|^2}{\sum_{k-N/2}^{N/2} \sum_{i,j=-M/2}^{M/2} \lambda(\mathbf{i}, \mathbf{j}) \left| k_{ijk}(0) \right|^2}. \quad (8)$$

Because $A(t)$ and $A'(t)$ reflect motion on a scale that is not intuitively related to true motion, it is necessary to "calibrate" the quality measures ($A(t)$ and $A'(t)$) with respect to "true" motion parameters (rotations and translations). As a measure of true motion for each time point, $S(t)$, we decided to calculate a weighted sum of the absolute parameters for a rigid-body transformation, which were obtained from the SPM realignment routine:

$$S(t) = \sum_{i=1}^{3} \left| x_i(t) \right| + \rho \left| \theta_i(t) \right|, \quad (9)$$

where the x_i represent x, y, and z translations, θ_i represent x, y, and z rotations, and ρ adjusts the relative weight between translations and rotations. Because our goal was to obtain 1 mm and 1° as cutoff, we conveniently set $\rho = 1$ (i.e., identical weight).

To determine whether the proposed quality measures $A(t)$ and $A'(t)$ can be used as an indicator for excessive motion, a set of 50 in vivo fMRI studies was analyzed. All scans were from subjects participating in an fMRI study that was approved by our local institutional review board. fMRI was performed on a 4-T Siemens/Varian MRI system, using a single-shot coronal gradient-echo EPI sequence (TR = 3000 ms, TE = 25 ms, FOV = 20 × 20 cm, 64 × 64 matrix size, 4-mm slice thickness, 1-mm gap, typically 33 slices). Each fMRI study contained 120 time frames, for a total raw data size of 130 Mb. All calculations were performed using the interactive data language (IDL, Research System, Inc., Boulder, CO). On a Compaq Alpha workstation XP 1000, the function $A(t)$, or $A'(t)$, for the time series described above, can be calculated in 5 s.

In order to obtain the $S(t)$ parameter described in Eq. (9),

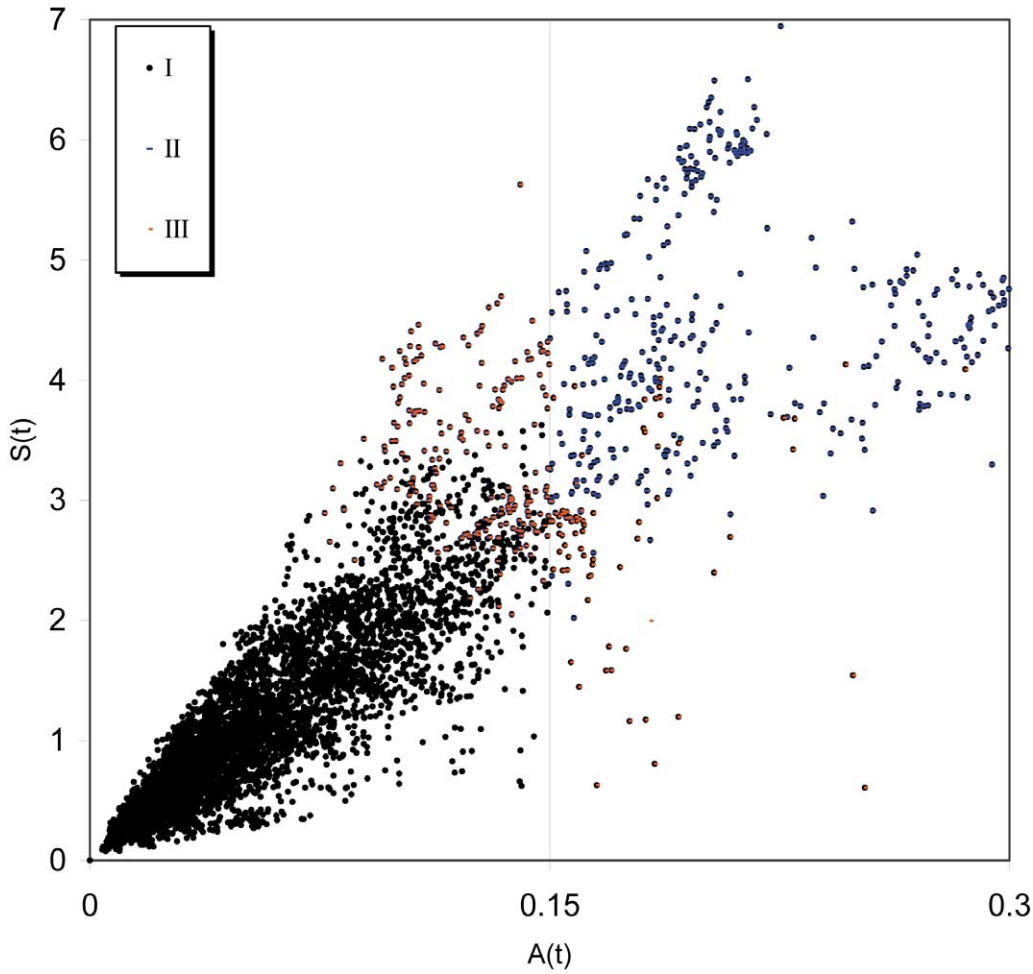

Fig. 6. Graph of $S(t)$ vs $A(t)$ for 6000 time points from 50 fMRI scans. *I*, correctly classified time points with motion <1 mm and <1°; II, correctly classified time points with motion >1 mm or >1°; III, time points with incorrect classification by the motion detector method ($N = 278$).

EPI images were reconstructed in IDL using a Hamming filter and a phase correction method that produced minimal ghost artifacts (Buonocore and Gao, 1997). The entire reconstruction step for an fMRI time series takes approximately 40 s. The reconstructed images were converted into SPM format, using AVS (Advanced Visual Systems, Inc., Waltham, MA). SPM99 was then used to realign the fMRI time series and to determine the six rigid-body motion parameters for calculating $S(t)$.

Results

The correlation between $A(t)$, or $A'(t)$, and $S(t)$ was excellent for the majority of the 50 fMRI studies evaluated (Fig. 3), with an average correlation coefficient of $r = 0.84$. The correlations were slightly better with a larger range of motion; for example, 85% of the 26 cases with unacceptable motion (>1 mm and >1°) had $r > 0.8$, versus 62% of the 24 cases with acceptable motion (<1 mm and <1°). However, excellent correlations (up to $r = 0.9$) were observed even for scans with very small motion. It is unlikely that this high degree of correlation is an artifact of activation-induced registration bias that has been observed for the SPM motion correction package (Freire et al., 2001, 2002). First, registration bias in SPM is significant for spatial smoothing with a full-width half maximum ≥8 mm, whereas our spatial smoothing (during image reconstruction) was approximately 2.5 mm. Second, our motion indicators did not show stimulus-related motion even when the range of motion was very small; for instance, Fig. 4 shows a scan with minimal motion but no correlation between $A(t)$ or $A'(t)$ and the stimulus profile (three activated and three resting periods of 20 time points each).

Figs. 4 and 5 exemplify the results from a scan with acceptable motion (translations <1 mm and rotations <1° on any axis; Fig. 4) and a scan with excessive motion (translations >1 mm and rotations >1° on all axes; Fig. 5). It is obvious that $A(t)$ and $A'(t)$ can be closely associated

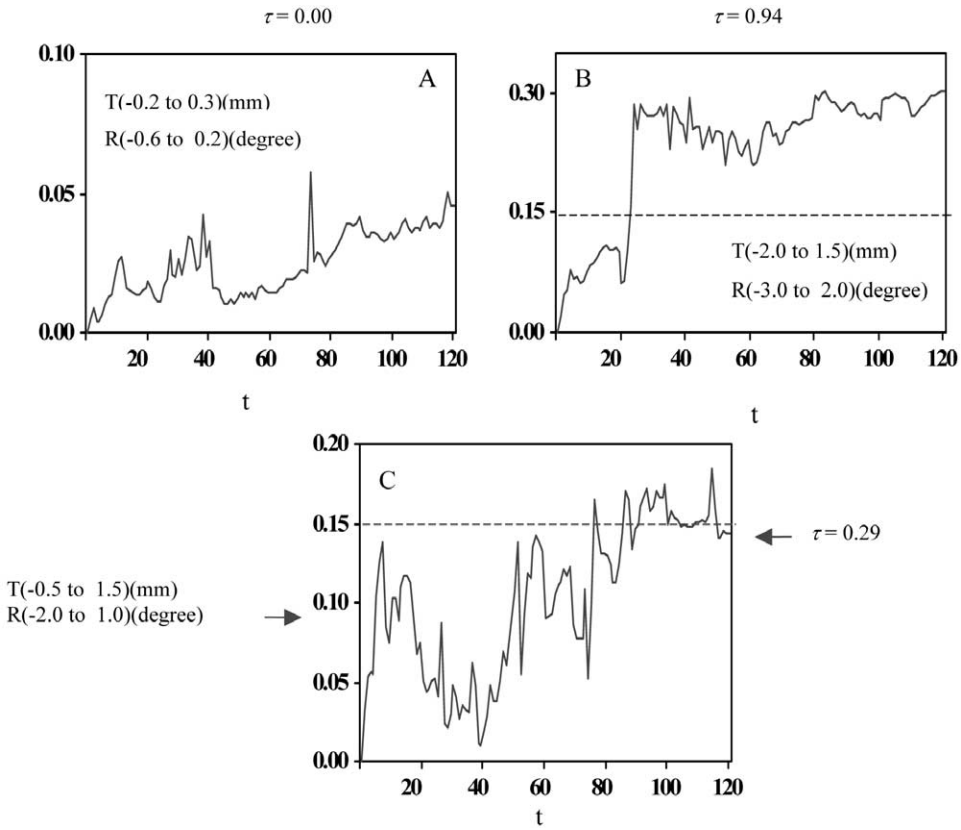

Fig. 7. Evolution of the quality parameter $A(t)$ during fMRI time courses. The values T and R represent the range of translations and rotations from SPM. (A) Motion substantially below threshold (0.15), accepted by our method; (B) excessive motion above the threshold, rejected by our method; and (C) motion close to the threshold, but rejected by our method because $\tau > 0.1$.

with one of the six SPM parameters in some cases (Fig. 5; $A(t)$ closely follows y translation and pitch), whereas this association becomes less obvious for other cases (Fig. 4). These two examples highlight the fact that the main goal is to derive a single parameter that indicates whether subject motion is acceptable or not, regardless of whether the underlying movement is a rotation or a translation, or of the specific axis of the movement.

Although Eq. (3) demonstrates that the quality function $A(t)$ is insensitive to in-plane translations, little qualitative differences were found between $A(t)$ and $A'(t)$. This apparent discrepancy is probably due to the fact that head translations in human fMRI studies are generally accompanied by rotations. Therefore, since $S(t)$ was better correlated with $A(t)$ than $A'(t)$ for almost all cases (see Fig. 3), only $A(t)$ will be used for the remainder of the paper.

The good correlation between the quality parameter $A(t)$ and the reference motion factor $S(t)$ from SPM suggests that it might be possible to define a single threshold value for $A(t)$ that classifies motion for a given scan to be acceptable or excessive. After evaluating $S(t)$ and $A(t)$ for all 50 fMRI time courses, $A(t) > 0.15$ was found to be the best indicator of excessive motion. Furthermore, we required a 10% tolerance in determining whether motion is excessive, where the tolerance τ is calculated as follows:

$$\tau = \frac{\sum_t B(t)}{\sum_t A(t)} \tag{10}$$

for

$$B(t) = \begin{cases} A(t) & \text{if } A(t) > 0.15 \\ 0 & \text{if } A(t) \leq 0.15 \end{cases}.$$

The use of the tolerance minimizes the frequency of false-negative cases in which the motion exceeded the threshold just marginally and for a few select time points.

The calibration of the motion detector was performed to accept or reject entire time series. Nevertheless, the proposed threshold provides good classification for single time points with regard to acceptable versus excessive motion; in fact, over 95% of all 6000 individual time points were classified correctly (Fig. 6). Furthermore, most individual points with incorrect individual classification belong to time series that were correctly classified by our method.

Fig. 7 demonstrates the practical use of the motion detector method. The line in each graph represents $A(t)$, and

the values T and R indicate the minimum and maximum translations and rotations determined with SPM99. Motion in Fig. 7A is subthreshold, with translations between less than 0.3 mm and rotations less than 0.6°. Accordingly, the quality parameter $A(t)$ is smaller than 0.1 for all time points, and $\tau = 0$. Fig. 7B shows the results in a subject that moved substantially (maximum translation 2 mm, maximum rotation 3°): the quality parameter $A(t)$ is above threshold (0.15) for most time points ($\tau = 94\%$). Finally, Fig. 7C shows an example with moderate amounts of excessive motion (translations up to 1.5 mm and rotations up to 2°). $A(t)$ is above threshold during the last part of the time series ($\tau = 29\%$), and the scan was rejected.

These results suggest that $A(t)$ might be used to identify subsets of scans that are acceptable for further analysis; for example, if unacceptable motion occurs only toward the end of a time series, the initial time points might still be valid for statistical analysis. This would require fMRI analyses with a variable number of time points for each scan; however, it is difficult and time-consuming to perform such analysis in existing analysis packages such as SPM, because a different design matrix must be created for each scan.

Across all 50 studies, the accuracy of the motion detector was 90%. The remaining 10% of incorrect classifications were all false-negative cases, i.e., scans that were deemed acceptable by the motion detector but that exceeded the threshold of motion according to SPM. However, all of these cases represent time series with marginal motion, in which motion parameters from SPM were close to 1 mm translation or 1° rotation. Of note, there were no false positives, i.e., scans where $A(t)$ detects excessive motion although subject motion is acceptable. This point is important, since false positives would result in unnecessary repeat scans.

Conclusion

A fast, *k*-space data-based algorithm was developed to detect and classify subject motion during fMRI time series. The algorithm determines the average squared difference between the first fMRI volume acquired and that of successive time points. Good agreement was found between our quality measure and the sum of the absolute values of SPM99 parameters of motion in 50 fMRI studies. The simple and fast algorithm achieves correct classification of excessive motion in 90% of all cases, with the remaining 10% showing marginally acceptable motion.

After development and calibration of the motion detector as described above, we applied the technique to over 100 additional fMRI studies to evaluate subject motion online. For these new scans, the performance of the motion detector was close to 100%. This has enabled us to provide highly accurate feedback to the subjects in real time whether their motion during the prior fMRI scans was acceptable or excessive and whether repeat scans with excessive motion are necessary.

Acknowledgments

This work was supported by grants from the NIMH (1R01 61427-01), NIDA (K24 DA16170), and the Biomedical Engineering Program of the DOE (OBER). Dr. D. Tomasi is a member of the Consejo Nacional de Investigaciones Cientificas y Técnicas, Argentina.

References

Buonocore, M.H., Gao, L., 1997. Ghost artifact reduction for echo planar imaging using image phase correction. Magn. Reson. Med. 38, 89–100.

Freire, L., Mangin, J.-F., 2001. Motion correction algorithms may create spurious brain activations in the absence of subject motion. NeuroImage 14, 709–722.

Freire, L., Roche, A., Mangin, J.-F., 2002. What is the best similarity measure for motion correction in fMRI time series? IEEE Trans. Med. Imaging 21, 470–484.

Friston, K.J., Ashburner, J., Frith, C.D., Poline, J.-B., Heather, J.D, Frackowiak, R.S.J., 1995. Spacial registration and normalization of images. Hum. Brain Mapp. 2, 165–189.

Friston, K.J., Williams, S., Howard, R., Frackowiak, R.S.J., Turner, R., 1996. Movement-related effects in fMRI time-series. Magn. Reson. Med. 35, 346–355.

Gradshteyn, I.S., Ryzhik, I.M., 1980. Table of Integrals, Series, and Products. Academic Press, New York.

Jenkinson, M., Bannister, P., Brady, M., Smith, S., 2002. Improved optimization for the robust and accurate linear registration and motion correction of brain images. NeuroImage 17, 825–841.

Jezzard, P., Balaban, R.S., 1995. Correction for geometric distortions in echo planar images from B_0 field variations. Magn. Reson. Med. 34, 65–73.

Mathiak, K., Posse, S., 2001. Evaluation of motion and realignment for functional magnetic resonance imaging in real time. Magn. Reson. Med. 45, 167–171.

Robson M.D., Gatenby J.C., Anderson A.W., Gore J.C., 1997. Practical considerations when correcting for movement-related effects present in fMRI time-series, in: Proceedings of the ISMRM, 5th Annual Meeting, Vancouver, BC, Canada, p. 1681.

Thesen, S., Heid, O., Mueller, E., Schad, L.R., 2000. Prospective acquisition correction for head motion with image-based tracking for real-time fMRI. Magn. Reson. Med. 44, 457–465.

Ward, H.A., Riederer, S.J., Grimm, R.C., Ehman, R.L., Felmlee, J.P., Jack Jr., C.R., 2000. Prospective multiaxial motion correction for fMRI. Magn. Reson. Med. 43, 459–469.

Welch, E.B., Manduca, A., Grimm, R.C., Ward, H.A., Jack Jr., C.R., 2002. Spherical navigator echoes for full 3D rigid body motion measurement in MRI. Magn. Reson. Med. 47, 32–41.

Wu, D.H., Lewin, J.S., Duerk, J.L., 1997. Inadequacy of motion correction algorithms in functional MRI: role of susceptibility-induced artifacts. J. Magn. Reson. Imaging 7, 365–370.